Method of Monitoring Three-dimensional Mining Surface Deformation Based on InSAR

Ling QUAN*, **Zijie LONG**, **Zongyao MA**, **Kangda CHEN**, **Xueliang CHEN**, **Yuanping XU**, **Jiale LIU**

College of Resource and Environment, Anhui Science And Technology University, Fengyang 233100, China

Abstract In order to solve the problems of small monitoring range, long time and high cost of existing sedimentation observation methods, based on two-view sentinel No. 1 radar images of Guqiao mining area in Huainan City from November 4, 2017 to November 28, 2017, surface change information was obtained in combination with D-InSAR, and the three-dimensional surface deformation was monitored by two-pass method and single line of sight D-InSAR method. The results show that during the research period of 24 d, the maximum deformation of the mining area reached 71 mm, and the southern subsidence was the most obvious, which was in line with the mining subsidence law. The maximum displacement from the north to the south was about 250 mm, while the maximum displacement from the east to the west was about 80 mm, and the maximum subsidence in the center was 110 mm. It is concluded that D-InSAR technique has a good effect on the inversion of the mining subsidence, and this method is suitable for three-dimensional surface monitoring in areas with similar geological conditions. The monitoring results have certain reference value.

Key words Synthetic aperture radar; Mining subsidence; Sentinel image; Two-pass method

DOI 10.19547/j.issn2152 - 3940.2024.01.013

After coal resources are extracted, goaf will be formed underground, causing a series of irreversible geological disasters such as house collapse[1], damage to transportation facilities[2], and reduction of land use area[3], as well as losses to the national economy. Therefore, it is necessary to strengthen the detection of the hollow area and grasp the subsidence rule in time.

Using InSAR technology to observe the settlement law has become the focus of many scholars at home and abroad. For instance, Abdikan *et al.* [4] conducted settlement monitoring on the edge of Zonguldak City, and proved that L band could reduce the influence of phase gradient. Wang Na *et al.* [5] used the two-pass method to process RADARSAT-2 data of a mining area in Shenmu County, and the result was highly similar to the analysis height of WorldView-2 high-resolution images. Abolghasem Goorabi *et al.* [6] monitored the landslides appearing in 2017, and detected the presence of aftershocks using Sentinel-1A data.

1 Technical principles of InSAR monitoring method

1.1 Principles of InSAR technology InSAR acquires three-dimensional surface deformation information by repeated observation of the same region by radar satellite[7], obtaining two images of the region and then the difference of surface deformation in different periods of the region.

The radar satellite repeatedly observes P point in different periods, transmits pulses and receives the reflected band intensity. The brightness values of SAR images in different bands are different.

$$h = H - R\cos\theta = H - \frac{B^2 - \left(\frac{\lambda}{4\pi}\varphi\right)^2}{\frac{\lambda}{2\pi}\varphi + 2B\sin(\theta - \alpha)}\cos\theta \tag{1}$$

In the formula, λ is radar wavelength; φ is the difference between echoes received by the radar; h represents the elevation of the earth's surface.

1.2 D-InSAR two-pass method The use of the two-pass method requires two-scene interference images and DEM[9]. The two SAR images have deformation δr in the direction of the observed oblique distance, and the interference phase φ_1 can be expressed as follows:

$$\varphi_1 = -\frac{4\pi}{\lambda}[(r_1 + \delta_r) - r_2] \tag{2}$$

2 Monitoring of D-InSAR mining subsidence

2.1 General situation of the study area Guqiao mining area is located in Fengtai County, Huainan City, Anhui province. The terrain of the whole mining area is flat, and it is slightly higher in the northwest than that the southeast. The mine was officially put into operation on April 28, 2007, and the designed annual output is 5 million t.

2.2 Types of data

2.2.1 SAR data. The data were the single view and complex ra-

Received: January 5, 2024 Accepted: February 16, 2024

Supported by the Talent Introduction Project of Anhui University of Science and Technology (ZHYJ202104); Horizontal Cooperation Project (881079, 880554, 880982); Innovation and Entrepreneurship Project of National College Students (S202310879289, S202310879296, X202310879098, X20231087-9097).

* Corresponding author.

dar images of sentinel No. 1 on November 4 and 28, 2017, and the data resolution was 5 m × 20 m.

2.2.2 DEM data. The SRTM3 DEM data adopted in this study were from NIMA and NASA, with a resolution of 90 m.

2.3 Monitoring of terrain deformation by the two-pass method

2.3.1 SAR data. Baseline estimation can evaluate the mass of the interference image pair, calculate the baseline, orbit offset, and other system parameters[4]. Estimation results: each 2π change of phase represented 0.028 m of settlement, and distance bias was 31.355 pixels, while azimuth bias was 7.319 pixels. Slope was 878 979.293 m, and time base was 24 d. Main image incidence was 39.580°, and space base was 85.575 m. Fig. 1 and Fig. 2 show the relationship between elevation and deformation accuracy and coherence, respectively. It is seen that elevation and deformation accuracy rose with the increase of coherence.

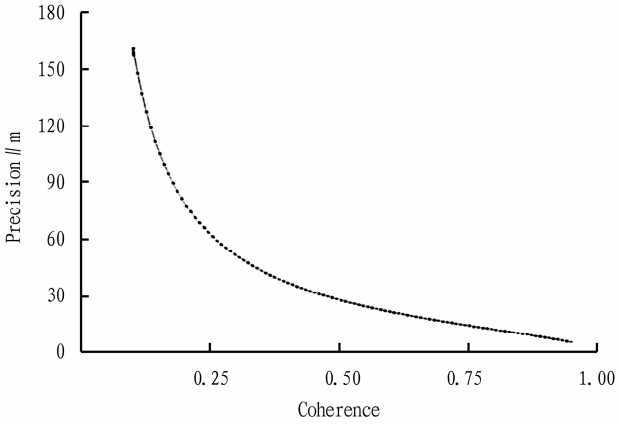

Fig. 1 Elevation accuracy and coherence

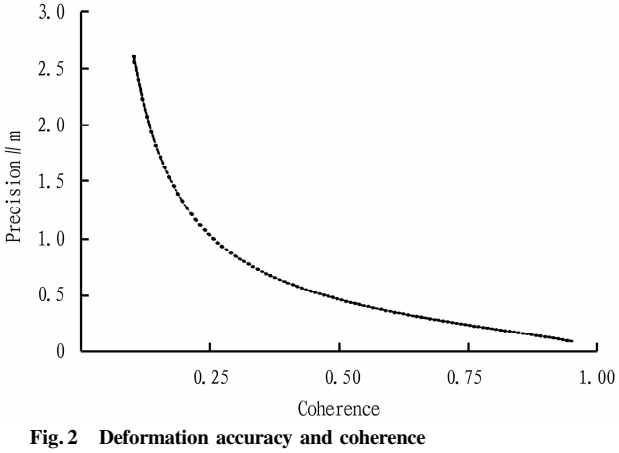

Fig. 2 Deformation accuracy and coherence

2.3.2 Experimental results. The results show that the interference fringe around the deformation area was relatively uniform, about 56 mm. The fringes in the study area were chaotic and distributed irregularly, and it was elliptical. Due to the large deformation in a short time, further analysis is needed. The poor coherence of the images may be due to the large changes in vegetation between November 4 and 28. In the study area belonging to a deciduous broad-leaved forest area, the vegetation coverage rate was higher on November 4, and the difference between the two periods was large, so the coherence was greatly affected. The shape variable of the study area was the largest. The subsidence was in an elliptical shape, increasing from the outer ring to the inner ring. The subsidence was the most serious in the northwest and gradually weakened in the southeast, which was in line with the actual driving process from northwest to southeast. The maximum settlement amount can reach 64 – 71 mm, and there was a wide range of subsidence throughout the whole working face; the settlement was funnel-shaped, according with the settlement law of mining settlement.

3 Three-dimensional surface deformation monitoring by the single line of sight D-InSAR

Surface mining subsidence includes horizontal and vertical movement, and the two-pass method can better detect the subsidence rate in the vertical direction, but cannot show the displacement in the horizontal direction. Based on the mining subsidence pattern, the single line of sight D-InSAR monitoring approach was adopted to make up for the shortcomings of the two-pass method.

3.1 Three-dimensional deformation extraction According to the subsidence law of the mining area and probability integral parameters, the settlement, east – west and north – south horizontal deformation fields in each monitoring period were extracted by using the prediction model. The settlement inversion diagram, the isocontours of horizontal movement from the east to the west and from the north to the south are shown in Fig. 3 – Fig. 5.

3.2 Analysis of results Fig. 3 shows the surface subsidence of the mine area, and the contour line means the settlement gradient. The outer settlement was 10 mm, increasing layer by layer. The central settlement was relatively large, up to 110 mm. It can be seen from Fig. 4 that the horizontal east – west movement of the studied mining area, and the deformation of the working face was roughly 20 – 40 mm. The maximum movement can reach 80 mm, and the maximum only existed in the local region. Fig. 5 shows the horizontal north – south displacement of the three-dimensional deformation. The maximum of the local displacement from the north to the south was 250 mm, and the deformation in the purple region was about 100 mm, while the surrounding displacement was about 50 mm. It indicates that the local bending in the north – south direction was large, while the overall deformation was small. From the inversion results of surface horizontal displacement and subsidence, it can be seen that the three-dimensional surface bending monitoring method based on the single line of sight D-InSAR has a good inversion effect, and this solution model is suitable for the terrain three-dimensional bending monitoring in Guqiao mining area of Huainan.

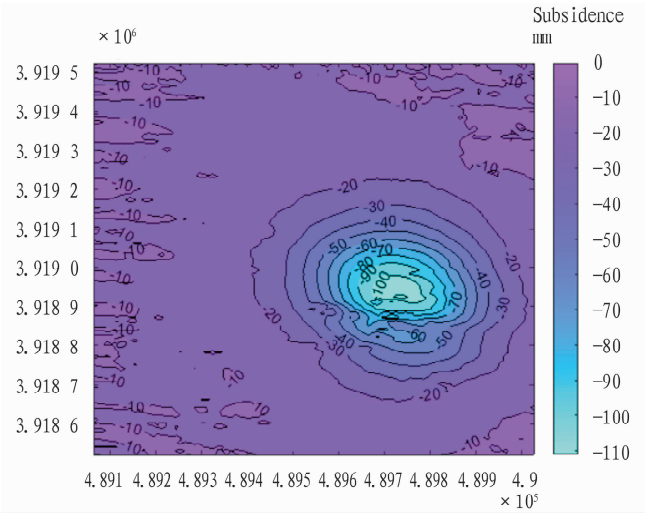

Fig. 3 Settlement diagram

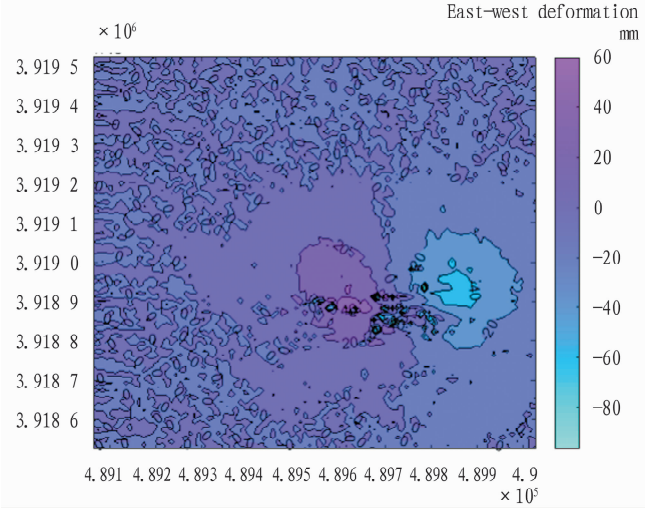

Fig. 4 Horizontal east – west movement

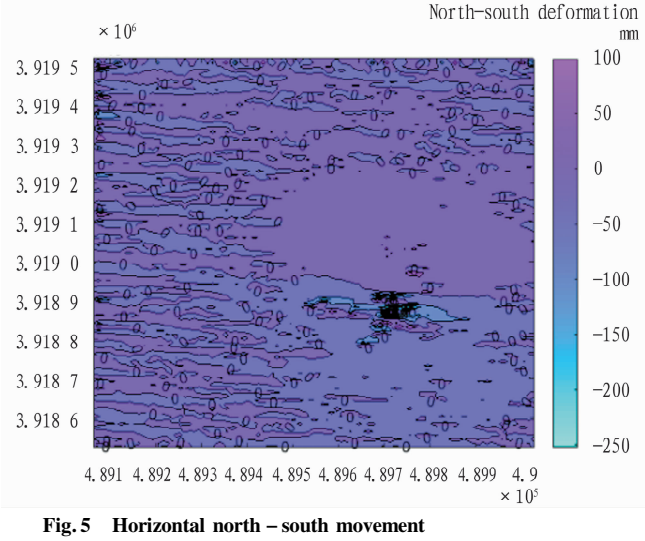

Fig. 5 Horizontal north – south movement

4 Conclusions

In this paper, the single line of sight D-InSAR technique and two-pass method were adopted to monitor the surface deformation of the mining area in the vertical direction during November 4 – 28, 2017. During the observation period, the maximum subsidence of the working face was 71 mm, and the south of the working face fell more seriously. Afterwards, the three-dimensional deformation of Guqiao mining area was monitored by using the single line of sight D-InSAR three-dimensional deformation extraction method. The maximum inversion subsidence was about 110 mm, and the maximum north – south horizontal displacement was about 250 mm, while the maximum east – west horizontal displacement was about 80 mm. The processing accuracy of data was high, meeting the requirements of engineering accuracy.

In this study, the two-pass method was combined with the single line of sight D-InSAR technology to construct the surface deformation extraction model of goaf, which can better invert the three-dimensional deformation of the study area, and has certain reference significance for the study of the law of settlement caused by the mining of mining areas with similar geological conditions.

References

[1] JIANG C. Research on theory, technology and application of three-dimensional mining subsidence monitoring based on InSAR[D]. Huainan: Anhui University of Science and Technology, 2022.

[2] LI Y, JIANG JX, DU YL, *et al.* Surface subsidence monitoring by time series InSAR integrating with distributed targets in mining region[J]. Journal of China University of Mining & Technology, 2020, 49(6): 1199 – 1206, 1232.

[3] WANG L, JIANG C, ZHANG XN, *et al.* Monitoring method of surface subsidence induced by inclined coal seam mining based on single line of sight D-InSAR[J]. Geomatics and Information Science of Wuhan University, 2019, 44 (6): 814 – 820.

[4] ABDIKAN S, ANKAN M, SANLI FB, *et al.* Monitoring of coal mining subsidence in peri-urban area of Zongguldak city (NW Turkey) with persistent scatterer interferometry using ALOS-PALSAR[J]. Environmental Earth Sciences, 2014, 71(9): 4081 – 4089.

[5] WANG N, XU SN, ZHOU JJ. Analysis of land subsidence in coal mining area based on DInSAR technology[J]. The Chinese Journal of Geological Hazard and Control, 2016, 27 (2): 110 – 114.

[6] ABOLGHASEM G. Detection of landslide induced by large earthquake using InSAR coherence techniques Northwest Zagros, Iran[J]. The Egyptian Journal of Remote Sensing and Space Sciences, 2020, 23(2): 195 – 205..

[7] CHEN YC, XU LJ, YU LR. The method of mining subsidence deformation monitoring and prediction based on D-InSAR with GIS technology [J]. Bulletin of Surveying and Mapping, 2019(7): 54 – 58, 63.

[8] LI N. Research on mining subsidence monitoring method based on single line of sight D-INSAR technology[D]. Huainan: Anhui University of Science and Technology, 2018.

[9] WEI C, FU BL, TAN JL, *et al.* Monitoring of spatial-temporal dynamic changes in water surface in marshes based on multi-temporal Sentinel-1A data[J]. Remote Sensing of Natural Resources, 2002, 34(2): 251 – 260.